An efficient platform for generating somatic point mutations with germline transmission in the zebrafish by CRISPR/Cas9-mediated gene editing

Received for publication, November 22, 2017, and in revised form, February 24, 2018 Published, Papers in Press, March 2, 2018, DOI 10.1074/jbc.RA117.001080

Yibo Zhang (張逸波), Zhiwei Zhang (張志偉), and Wei Ge (葛偉)[1]

From the Centre of Reproduction, Development and Aging (CRDA), Faculty of Health Sciences, University of Macau, Macau 999078, China

Edited by Xiao-Fan Wang

Homology-directed recombination (HDR)–mediated genome editing is a powerful approach for both basic functional study and disease modeling. Although some studies have reported HDR-mediated precise editing in nonrodent models, the efficiency of establishing pure mutant animal lines that carry specific amino acid substitutions remains low. Furthermore, because the efficiency of nonhomologous end joining (NHEJ)-induced insertion and deletion (indel) mutations is normally much higher than that of HDR-induced point mutations, it is often difficult to identify the latter in the background of indel mutations. Using zebrafish as the model organism and Y box–binding protein 1 (Ybx1/*ybx1*) as the model molecule, we have established an efficient platform for precise CRISPR/Cas9-mediated gene editing in somatic cells, yielding an efficiency of up to 74% embryos. Moreover, we established a procedure for screening germline transmission of point mutations out of indel mutations even when germline transmission efficiency was low (<2%). To further improve germline transmission of HDR-induced point mutations, we optimized several key factors that may affect HDR efficiency, including the type of DNA donor, suppression of NHEJ, stimulation of HDR pathways, and use of Cas9 protein instead of mRNA. The optimized combination of these factors significantly increased the efficiency of germline transmission of point mutation up to 25%. In summary, we have developed an efficient procedure for creating point mutations and differentiating mutant individuals from those carrying knockouts of entire genes.

With the recent development of genome editing technologies, in particular transcription activator-like effector nuclease (TALEN)[2] and clustered regularly interspaced short palindromic repeats (CRISPR) and CRISPR-associated nuclease 9 (Cas9) (CRISPR/Cas9), numerous genes in a large number of species have been knocked out *in vitro* and *in vivo* for functional analysis and disease modeling (1–5). However, the nonhomologous end joining (NHEJ)–induced whole gene disruption cannot fully dissect the details of gene functions such as the importance of specific posttranslational modifications (6–8). Clinical studies have shown that many genetic disorders are caused by point mutations affecting single amino acids instead of whole gene disruption. For instance, mutations of Kras G12V and Braf V600E occur in over 50% of cancer patients (9). Single amino acid substitutions in these two genes typically result in constitutive activation of Kras and Braf, which cannot be mimicked by knockout of the whole gene (10, 11). Therefore, substitution for single amino acid is essential for studying gene function and disease modeling. Although much effort has been spent recently, site-directed point mutation *in vivo* still remains a challenging task. The technical bottlenecks for homology-directed recombination (HDR)–mediated site-specific mutagenesis are low efficiency (12–15), and it is difficult to differentiate the point mutants from the insertion and deletion (indel) mutations (16–19). This issue has been addressed by some recent studies (12, 20, 21). One of the key factors explored to increase HDR efficiency is the type of donor DNA (18, 22). However, the results have so far been controversial and inconsistent. It has recently been reported that Cas9 asymmetrically releases the 3′-end of the cleaved DNA strand, which is not annealed to the single guide RNA (sgRNA) before complete dissociation of the Cas9 protein. Therefore, asymmetrical single-stranded DNA (ssDNA) donors exhibited a five-time higher efficiency *in vitro* than others (up to 55%) (23). In contrast, another study using double-stranded DNA (dsDNA) donor also reported a high mutation efficiency *in vivo* (46%) (17). These results suggest that the choice of ssDNA and dsDNA may be sequence-dependent. The second strategy to improve HDR efficiency is to suppress the activity of NHEJ pathway with SCR7, an inhibitor of DNA ligase IV that joins ends of DNA breaks (24–26), or to increase the activity of HDR pathway with RS-1, a stimulator of Rad51 that promotes HDR (27, 28). SCR7 has been reported to improve HDR efficiency by 4- to 6-fold in cultured cells and up to 19-fold in mice (29, 30), whereas the application of RS-1 resulted in a 2–5-fold increase of HDR efficiency *in vitro* (27).

This study was supported by University of Macau Grants MYRG2014-00062-FHS, MYRG2015-00227-FHS, MYRG2016-00072-FHS, and CPG2014-00014-FHS and The Macau Fund for Development of Science and Technology Grants FDCT114/2013/A3 and FDCT/089/2014/A2 (to W. G.). The authors declare that they have no conflicts of interest with the contents of this article.

This article contains Figs. S1–S5 and Table S1.

[1] To whom correspondence should be addressed. Tel.: 853-88224996; Fax: 853-88222314; E-mail: weige@umac.mo or gezebrafish@gmail.com.

[2] The abbreviations used are: TALEN, transcription activator-like effector nuclease; Cas9, CRISPR-associated nuclease 9; NHEJ, nonhomologous end joining; HDR, homology-directed recombination; indel, insertion and deletion; sgRNA, single guard RNA; ssDNA, single-stranded DNA; DSBs, double-strand breaks; HRMA, high-resolution melting analysis; qPCR, quantitative PCR; PGC, primordial germ cells.

© 2018 by The American Society for Biochemistry and Molecular Biology, Inc. Published in the U.S.A.

In the past 20 years, zebrafish have become a popular model for reverse genetic analysis of vertebrate development and human diseases (15, 19, 31–34). Similar to other model organisms, zebrafish are amenable to genetic manipulation because of their small size, short life cycle, and high fecundity (33). These biological advantages together with their sharing 70% human genes and 84% human genetic disease genes (35) have made zebrafish one of the top choices for basic study of gene function and modeling of human genetic diseases as well as drug screening (36). Because of this, zebrafish have often been a platform for testing and optimizing protocols of genome editing in recent years. A large number of genes have been knocked out in zebrafish by using zinc finger nuclease (ZFN), TALEN, or CRISPR/Cas9 (37). A few studies have also been reported on HDR-mediated point mutations (13, 15, 18, 36, 38); however, the efficiency is generally very low.

In the present study, we attempted to develop a standard platform using zebrafish as the model to introduce HDR-mediated point mutations *in vivo* with high efficiency, and to differentiate these mutants from those carrying random indel mutations. We used Y box–binding protein 1 (YB-1; Ybx1/*ybx1*) as the model molecule. Ybx1 is a multifunctional protein, and its functions depend on its subcellular location, which is regulated, at least partly, by the phosphorylation at Ser-102 in humans (39). Our unpublished work has shown that Ybx1 may likely be a critical regulator in controlling ovarian follicle development, and the phosphorylation of its Ser-82 (equivalent to Ser-102 in humans) appears to play a critical role in its function.[3] We therefore chose Ser-82 as the target site in the present study to test the efficiency of HDR-mediated mutagenesis and our screening strategy.

Results

Designing of target sites for site-directed mutagenesis for zebrafish Ybx1^{S82A} in vivo

As the first step toward precise point mutation, we identified one potential TALEN and two CRISPR/Cas9 targets by the online ZiFiT Targeter software (http://zifit.partners.org/ZiFiT)[4] (64, 65). Genotype analysis on the injected embryos showed that all sites worked but with varying efficiency. The mutation rates (percentage of embryos that carried mutations) of the two CRISPR sites were ~30 and 80% for sites 1 and 2, respectively, whereas the efficiency of the TALEN site was 30% (Fig. S1). Because the efficiency of HDR is highly dependent on the efficiency of double-strand breaks (DSBs) (14, 40), we chose no. 2 CRISPR site for further experiments on HDR-mediated mutagenesis.

Optimization of DNA donors for HDR-mediated point mutation

To optimize the condition for site-directed mutagenesis, we compared the efficiency of three different DNA donors: ssDNA, dsDNA, and plasmid (Fig. 1*B*). The ssDNA donor was synthesized by Integrated DNA Technologies (IDT), whereas dsDNA and plasmid donor were assembled using fusion PCR and TA cloning (Fig. 1*C*). The mutation region of the donor included the mutated sequence to recode Ser-82 to Ala-82 and blocking mutations to prevent the cleavage of donor DNA by CRISPR/Cas9 and retargeting of the site by sgRNA/Cas9 complex (Fig. 1*B*). These blocking mutations were also helpful for designing the mutant-specific primer because the conventional high-resolution melting analysis (HRMA) is unable to distinguish HDR mutations from different types of indel mutations. The mutant-specific primer recognizes HDR-induced mutation only so as to eliminate all random indel mutations and the WT sequence. To avoid interference by the residual donor DNA, we designed a pair of primers (F1/R1) that are located outside the region of the donor DNA for the first round of nested PCR (Fig. 1*D*). The typical result of nested real-time quantitative (qPCR) screening with F2 and mutant-specific R2 is shown in Fig. 2*A*. The primer R2 was highly specific to HDR-induced mutation, and it did not amplify the WT sequence and indel mutants. The positive samples were also confirmed by sequencing (Fig. 2*B*). Although some studies reported that ssDNA was more effective than dsDNA and plasmid donors (12, 41–44), ssDNA showed the lowest efficiency in this study. By comparison, the plasmid donor showed the highest efficiency (15–16%) compared with dsDNA (8–10%) and ssDNA (0–5%). The efficiency of NHEJ-mediated indel mutation remained almost the same for all three DNA donors (Fig. 2*C*).

Effects of suppressing NHEJ and stimulating HDR on HDR-mediated point mutation

Because DSBs induced by target-specific nuclease (Cas9 in CRISPR and FokI in TALEN) can be repaired by both NHEJ and HDR pathways, it is hypothesized that suppressing the NHEJ pathway may likely increase the efficiency of HDR (30). To demonstrate this, we treated the injected embryos with SCR7 (20 μM), an inhibitor of NHEJ. The concentration of 20 μM was used because it showed the lowest toxicity to the embryos while achieving the highest possible mutation efficiency (Fig. S2*A*). Our result, for the first time, showed that SCR7 significantly improved the HDR efficiency in the zebrafish for all three kinds of DNA donors in both Cas9 mRNA– and Cas9 protein–injected groups. For ssDNA donor, SCR7 increased HDR efficiency from 0 to 3% with Cas9 mRNA and from 5 to 13% with Cas9 protein. For dsDNA, the increase was from 8 to 22% and 10 to 25%, respectively. Among these DNA donors, the plasmid donor again showed the highest efficiency of point mutation in the presence of SCR7. The mutation rate increased from 16 to 58% and from 15 to 55%, respectively, for Cas9 mRNA and protein (Fig. 2*C*).

Apart from suppressing the NHEJ pathway, stimulation of the HDR pathway may also increase the efficiency of HDR (27). To test this, the embryos injected with sgRNA, plasmid donor, and Cas9 protein were incubated in the water containing RS-1 (20 μM), a Rad51 stimulator (28). Again, the concentration used was optimized for low toxicity and high mutation efficiency (Fig. S2*B*). The result showed that RS-1 significantly improved the HDR efficiency (15% to 24%), although its effect was weaker than SCR7. Moreover, we demonstrated, for the first time, that

[3] L. Zhang, Z. Zhang, B. Zhu, M. A. Sun, S. M. Ngai, and W. Ge, unpublished results.

[4] Please note that the JBC is not responsible for the long-term archiving and maintenance of this site or any other third party hosted site.

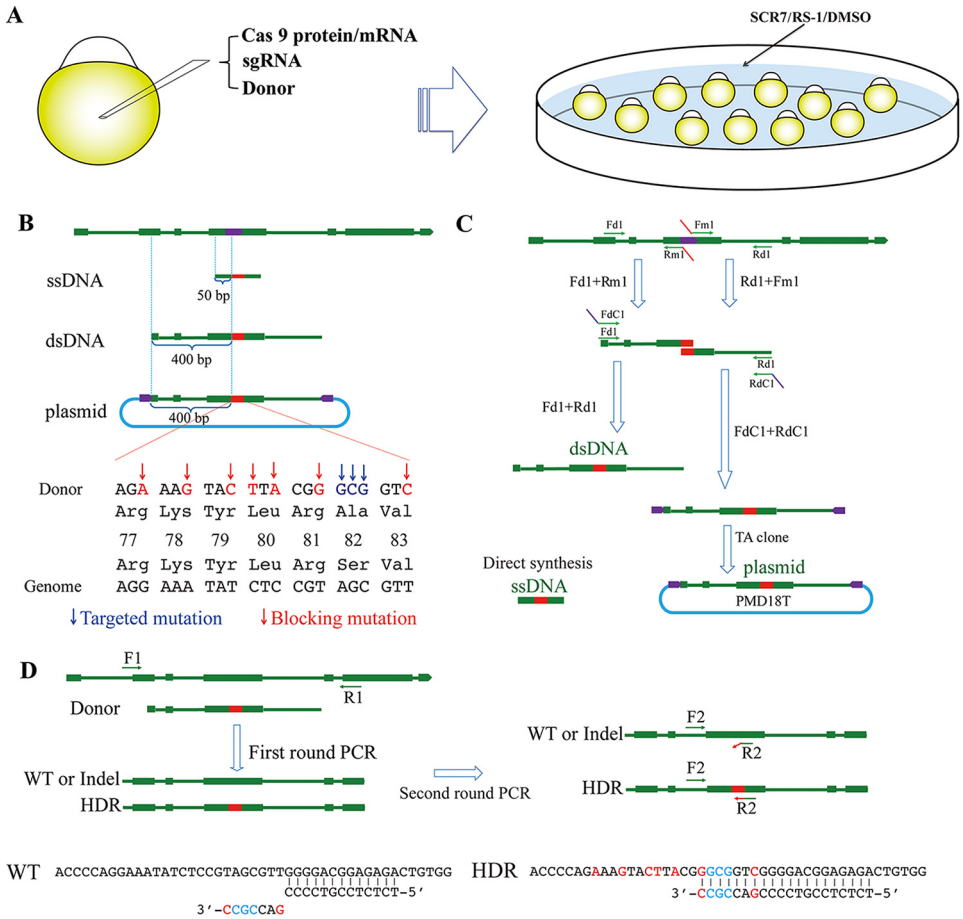

Figure 1. Schematic illustration of DNA donor construction for HDR-induced substitution of S82A in zebrafish Ybx1 (Ybx1^{S82A}). *A*, scheme of microinjection and treatment with SCR7 (NHEJ inhibitor) and/or RS-1 (HDR stimulator). A total volume of 4.6 nl Cas9 protein/mRNA (200 ng/μl), sgRNA (50 ng/μl), and DNA donor (200 ng/μl) mixture was injected into the yolk of 1-cell embryos. The injected embryos were then incubated in 20 μM SCR7 and RS-1 alone or in combination for 6 h. DMSO was used as the vehicle control. *B*, design of DNA donors for targeted substitution of Ala-82 for Ser-82 (S82A). The blocking mutations were introduced to prevent retargeting of the edited sequence by sgRNA. *C*, generation of different donors for S82A substitution. The ssDNA donor was synthesized by IDT directly. For dsDNA donor, the left and right homology arms were amplified from the zebrafish genome DNA using primer pairs Fd1+Rm1 (*left*) and Fm1+Rd1 (*right*). Fm1 and Rm1 carried targeting and blocking mutation sequences at the 5′-end. The left and right homology arms were then assembled by fusion PCR using the primers Fd1+Rd1. For the plasmid donor, the left and right homology arms were similarly amplified from the zebrafish genome DNA except that FdC1 and RdC1 primers used carried the CRISPR site and PAM sequence at the 5′-end. The product of fusion PCR was inserted into the plasmid by TA cloning. Both dsDNA and plasmid were sequenced to ensure no mutations introduced by PCR amplification. *D*, genotyping for HDR-induced S82A substitution. Primer F1 and R1 are located outside the donor regions, and primer F2 is located 50 bp upstream of the mutant sequence. Primer R2 is specific for HDR-induced mutation, and its 3′-end can only recognize the S82A mutant sequence without binding to WT and indel mutant sequences.

the combination of SCR7 and RS-1 further increased the HDR efficiency to 74%, showing an additive effect (Fig. 2*D*). Further experiment showed that SCR7 reduced NHEJ-mediated indel mutation in the absence of DNA donors. Interestingly, RS-1 alone had no such effect, but it could enhance the inhibitory effect of SCR7 when they were applied together (Fig. S3). However, no significant effects were observed in the presence of DNA donors (Fig. 2*D*).

Comparison of Cas9 mRNA and protein in inducing HDR

In mice, it takes 2 days for the embryos to develop from 1-cell to 8-cell stage (45); in the zebrafish, this process finishes within 75 min. Therefore, the time for Cas9 translation and assembly of Cas9 and sgRNA may not be critical for genome editing in mice because of its slow embryonic development. However, this could be critical for gene editing in the zebrafish with fast cell division and development. We therefore hypothesized that direct introduction of Cas9 protein in the zebrafish could make a significant difference from using Cas9 mRNA. To provide evidence for this idea, we first examined the temporal patterns of Cas9 protein in the embryos injected with Cas9 protein or mRNA. As shown in Fig. 3*A*, Cas9 protein could be detected in 1-cell embryos immediately after injection with the protein, and it lasted until 32-cell stage. In contrast, no Cas9 protein could be detected in the Cas9 mRNA–injected embryos from 1- to 4-cell stage. A weak signal started to appear in 8-cell embryos and the signal increased steadily afterward, reaching the highest at 32-cell stage, which was the last sampling point (Fig. 3*A*). It should be noted that in Cas9 protein–injected embryos, there was a progressive increase of the protein from 1- to 4-cell stage. This was likely because of some loss of the protein during the de-yolk step of sample preparation. We injected Cas9 mRNA and protein in the yolk mass, and it takes some time for them to migrate out of the yolk region.

To figure out the time window of HDR occurrence in Cas9 mRNA– and protein–injected embryos, we used nested PCR to

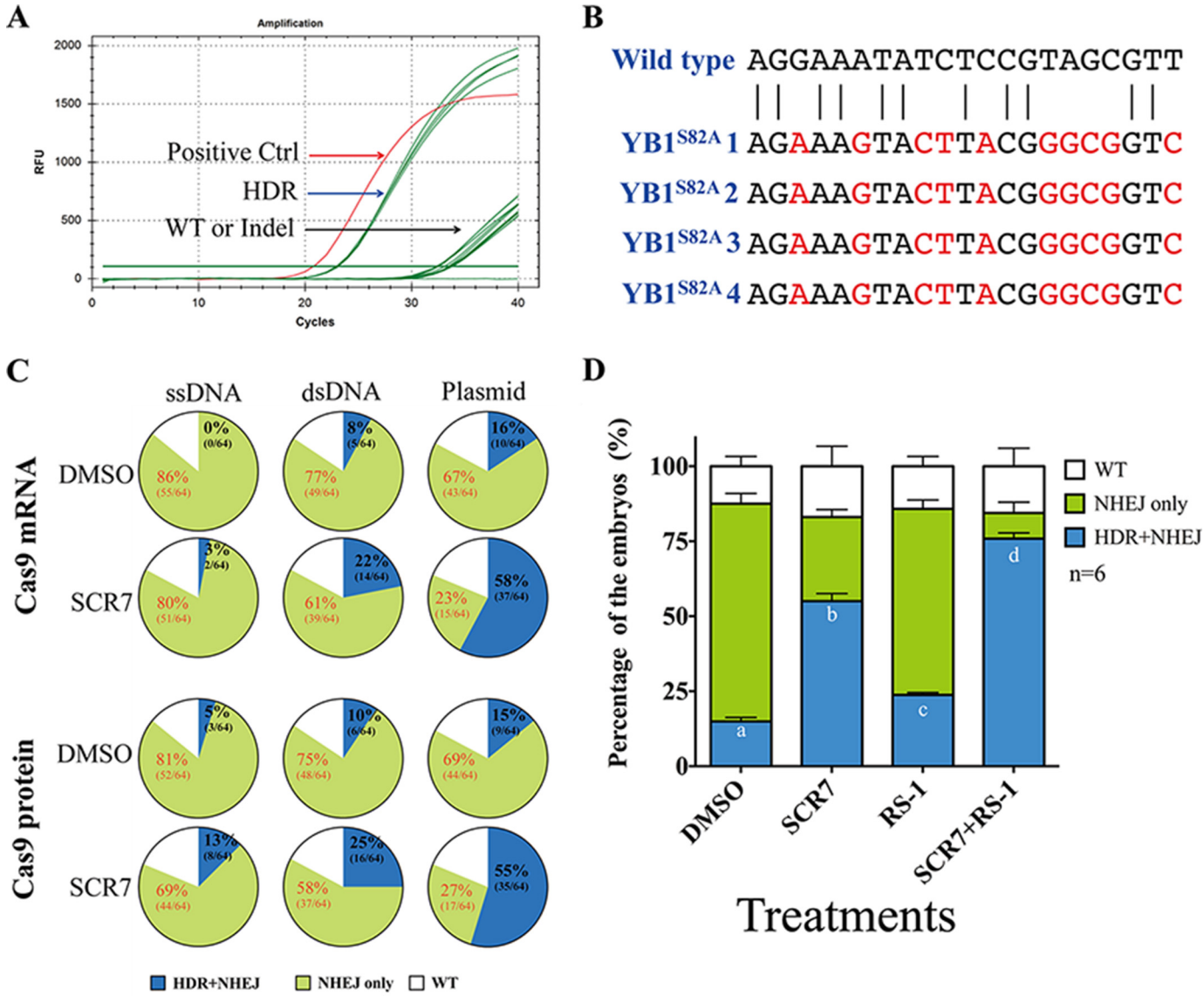

Figure 2. Optimization of conditions for efficient site-directed mutagenesis for Ybx1^{S82A}. *A*, representative real-time qPCR to distinguish Ybx1^{S82A} from WT and random indel mutations. Nested qPCR (F1/R1 for the first round, and F2/R2 for the second round) was performed on DNA extracted from embryos to avoid interference by the residual donor DNA. *B*, four mutant individuals identified by mutant-specific primers (F2/R2) in real-time qPCR. The identity of these individuals was confirmed by sequencing the amplicons produced with primers F4/R4 (see Fig. 6*A*) that flank the mutated region. *C*, efficiency of HDR-mediated point mutation for Ybx1^{S82A} and NHEJ-mediated indel (using primers F0/R0, see Fig. S1) with different DNA donors and Cas9 (mRNA *versus* protein) in the presence or absence of SCR7 (NHEJ inhibitor). One-cell embryos were injected with 4.6 nl solution containing sgRNA (50 ng/μl) and Cas9 mRNA or protein (200 ng/μl). The injected embryos were then incubated in 20 μM SCR7 or equal amount of vehicle DMSO as control for 6 h. In total, 64 injected embryos were analyzed for each treatment. *D*, effect of RS-1 (HDR stimulator) on HDR-mediated point mutation and NHEJ-mediated indel (using primers F0/R0). Similar to the treatment with SCR7, the embryos injected with Cas9 protein were incubated in 20 μM RS-1 in the presence or absence of 20 μM SCR7 for 6 h. The values are mean ± S.E. of six independent breeding experiments using different fish (n = 6). In each breeding, we sampled 24–32 embryos for analysis.

detect the existence of the earliest HDR during embryonic development (Fig. 3*B*). Because the product of the first-round PCR (F3/R3) was used as template for the second round directly without dilution, we used the primers F1/R1, also outside the donor, for the second-round PCR to exclude interference by the donor. As shown in Fig. 3*C*, the HDR was first detected with F1/R2 in 16-cell embryos injected with Cas9 protein, whereas in Cas9 mRNA–injected embryos, HDR was first detectable in 128-cell embryos, three cell cycles later than that injected with Cas9 protein. To assess overall mutation efficiency, we digested the amplification products of F1/R1 with T7 endonuclease I (T7E1 assay) to detect all potential mutations including indels and HDR. Results showed that mutations could be detected in 2-cell embryos injected with Cas9 protein. However, no HDR-induced point mutation could be detected at this stage with mutation-specific primer R2, suggesting that the mutations detected by T7E1 were mostly because of NHEJ-mediated random indels. In contrast, the NHEJ-induced mutations were first detected in 16-cell embryos injected with Cas9 mRNA. These results indicated that NHEJ occurred one cell cycle after the appearance of Cas9 protein in cells, which was 2-cell and 16-cell stage for Cas9 protein– and mRNA-injected embryos, respectively (Fig. 3*D*). For HDR-mediated point mutation, it was first detected with mutant-specific primer R2 in 16-cell embryos injected with Cas9 protein, and 128-cell embryos injected with Cas9 mRNA. Collectively, these data showed that both NHEJ

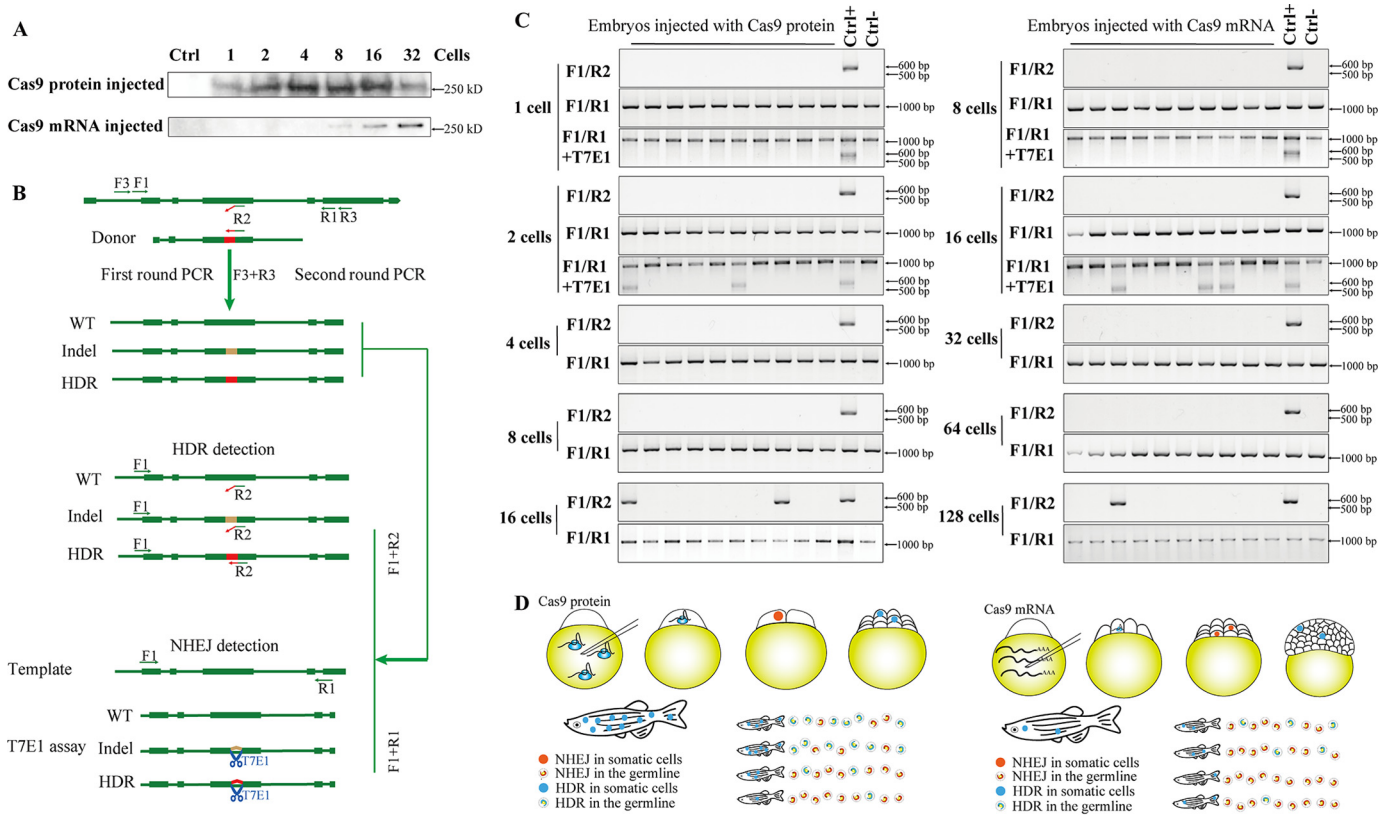

Figure 3. Cas9 protein *versus* mRNA in HDR-induced point mutation and NHEJ-mediated indel mutation. *A*, presence of Cas9 protein at different developmental stages of zebrafish embryos injected with Cas9 mRNA or protein. Each sample was prepared from 50 embryos of the same stage. The proteins were mostly extracted from the animal pole after removing the chorion and yolk. *B*, schematic illustration of genotyping strategy with nested PCR for HDR-mediated point mutation of Ybx1^{S82A} and NHEJ-mediated random indel mutations. In the first round of reaction, primers F3 and R3 located outside the donor DNA region were used to avoid interference by residual donor DNAs. The products of this round of PCR would include all possible sequences (WT, indel mutations, and point mutation) and were used either for T7E1 assay or the second round of PCR for HDR detection. Primers F1 and R2 (mutant-specific) were used in the second round of reaction for detecting HDR mutation only. *C*, detection of NHEJ-induced indel mutations (T7E1 assay on PCR products with F1/R1) and HDR-mediated point mutation (PCR with F1/R2) during early embryonic development. *D*, schematic illustration of temporal patterns of NHEJ-induced indel mutations and HDR-mediated point mutation in both somatic cells and germlines with either Cas9 protein or mRNA.

and HDR were advanced for three cell cycles by direct introduction of Cas9 protein as compared with those with Cas9 mRNA, and that HDR took place about three cell cycles behind that of NHEJ.

It is believed that the earlier the mutation occurs in the embryonic development, the more organs or tissues will carry such mutation in adults. To test this idea, we sacrificed nine F0 founders that showed germline transmission of HDR mutation (#1–7 from Cas9 protein–injected group and *1–2 from Cas9 mRNA–injected group) (see below for details on germline screening) and five fish that were shown to carry the mutation by caudal fin genotyping but failed to transmit the mutation to the next generation (#8–9 from Cas9 protein–injected group and *3–5 from Cas9 mRNA–injected group) (Fig. 4). Genomic DNA was isolated from the heart, gut, liver, gill, kidney, eye, muscle, gonad, as well as the caudal fin, followed by genotyping with HRMA. As shown in Fig. 4*A*, the HDR-induced mutation showed mosaic patterns in all fish examined. It was obvious that the Cas9 protein group showed higher rates of somatic mutation than Cas9 mRNA group, especially for HDR-induced S82A point mutation (Fig. 4*A*). The result also suggests that genotyping with caudal fin DNA can help enrich the founders carrying mutations; however, it cannot guarantee germline transmission, as shown by fish #8–9 and *3–5. On the other hand, a negative result with caudal fin genotyping cannot rule out the possibility of germline transmission, as shown by fish #6–7 and *1–2 (Fig. 4*B*). It is interesting to note that the germline transmission rates for HDR-induced point mutations were highly variable between individuals; however, the transmission rates for total mutations (HDR and NHEJ) remained relatively constant (Fig. 4*B*).

Establishment of screening protocol for differentiating HDR-mediated point mutations from NHEJ-induced indel mutations

Germline transmission is critical for establishing stable mutant lines. The most challenging issue in creating single amino acid substitution is to differentiate HDR-induced point mutations from a large number of NHEJ-induced indel mutations, which are much more frequent in F1 generation. The methods reported so far such as HRMA and T7E1 assay are commonly used for screening mutations, but they are ineffective in distinguishing HDR-induced point mutations in F1 generation from random indel mutations (19, 36).

Herein, we developed a simple and effective procedure for screening germline transmission of HDR-induced point mutations. As the first step of screening, we performed a mass breeding using the iSpawn (Tecniplast) with all F0 individuals regard-

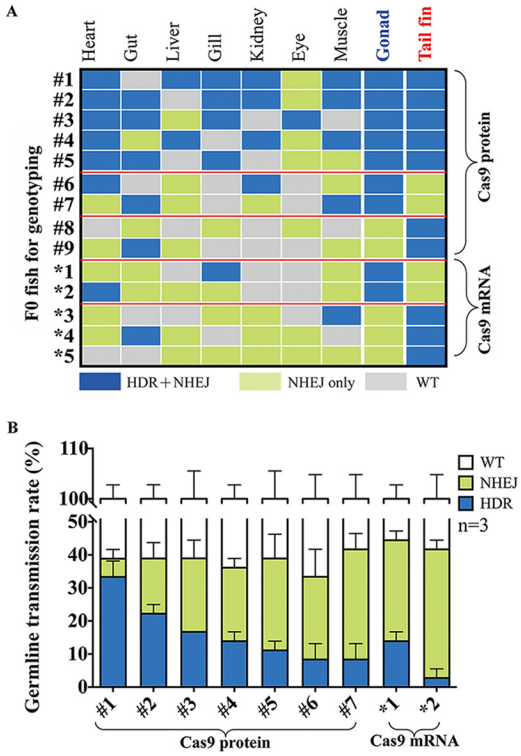

Figure 4. Tissue/organ distribution of Ybx1^{S82A} mutation in F0 founders and germline transmission. *A*, Ybx1^{S82A} mutation and NHEJ-mediated indel in different organs of F0 founders injected with Cas9 mRNA or protein. Primers F2 and R2 (see Fig. 1) were used for screening HDR-induced Ybx1^{S82A} mutation, and primers F0 and R0 (see Fig. S1) were used for screening NHEJ-mediated indel. Different organs were dissected from 9 F0 individuals injected with Cas9 protein (#1–9) and 5 individuals injected with Cas9 mRNA (*1–5) for genotyping. *B*, germline transmission rate (percentage of F1 mutant embryos) for Ybx1^{S82A} mutation and NHEJ-mediated indel mutations in 7 founders injected with Cas9 protein (#1–7) and 2 founders injected with Cas9 mRNA (*1–2). For each test, 12 embryos were collected for genotyping, and three independent breeding tests were performed for each individual. The values are mean ± S.E. of three experiments (n = 3).

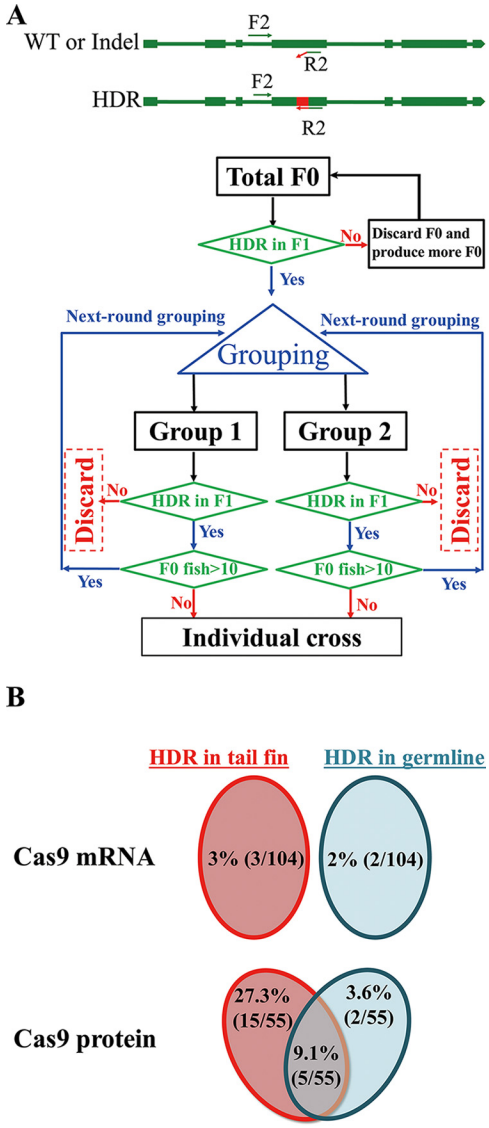

Figure 5. Screening strategy for germline transmission of Ybx1^{S82A} mutation. *A*, schematic illustration of the screening strategy for identifying F0 founders with germline transmission of Ybx1^{S82A} mutation. Because residual donor DNAs did not exist in the F1 embryos, we used primers F2 and R2 directly without nested PCR. All F0 founders carrying indel mutations in the tail fin were placed in the iSpawn for mass breeding. About 1000–3000 embryos were collected for each round of breeding. Small breeding tanks were used for breeding 2 to 10 F0 fish, and about 200–800 embryos were collected for each round of breeding. Fifty embryos were pooled together for genomic DNA extraction and genotyping. *B*, improvement of HDR-induced Ybx1^{S82A} mutation in the germline and reliability of caudal fin genotyping in identifying F0 founders injected with Cas9 protein. The HDR-induced Ybx1^{S82A} mutation was detected with primer pair F2/R2.

less of being positive or not in caudal fin genotyping assay. The F1 embryos were collected and divided into groups of different numbers (10–100/group) for genomic DNA extraction and qPCR assay with mutant-specific primer R2 (F2/R2) (Fig. 5*A*). As shown in Fig. S4, the highest number of embryos per group that generated specific signal was 50. Therefore, in our future screening, we pooled no more than 50 F1 embryos per group for initial screening. In the experiment shown in Fig. 5*B* and Fig. S4, we obtained 104 F0 founders injected with Cas9 mRNA. Three fish were found to carry mutations in the tail; however, they showed no germline transmission (*3–5) (Fig. 4). The remaining 101 F0 fish were subject to stepwise mass breeding and screening as described above. In the first cycle of mass breeding, we analyzed 47 samples (2350 F1 embryos in total) from these 101 F0 founders and confirmed that this pool of founders contained germline transmission of S82A. We then divided the initial pool of F0 fish into two groups for group breeding and found that one group (50 fish) contained S82A mutation (35 samples, 1750 embryos analyzed) in the germline. Further grouping and screening was performed and repeated for this group (23 samples, 1150 embryos for each round of screening). After four rounds of grouping and screening, one final group of 5 F0 founders was found to carry S82A mutation in their germlines. These fish were crossed individually with a WT fish and their offspring screened with mutant-specific PCR (11 samples, 550 embryos for each individual). Using this approach, we finally identified 2 F0 fish from 101 founders that contained HDR-induced point mutation of S82A (Ybx1^{S82A}) in the germline (Fig. S4).

Comparison of Cas9 mRNA and protein in promoting germline transmission of HDR-induced point mutation

With the protocol established for identifying F0 fish with germline transmission of HDR-induced single point mutation,

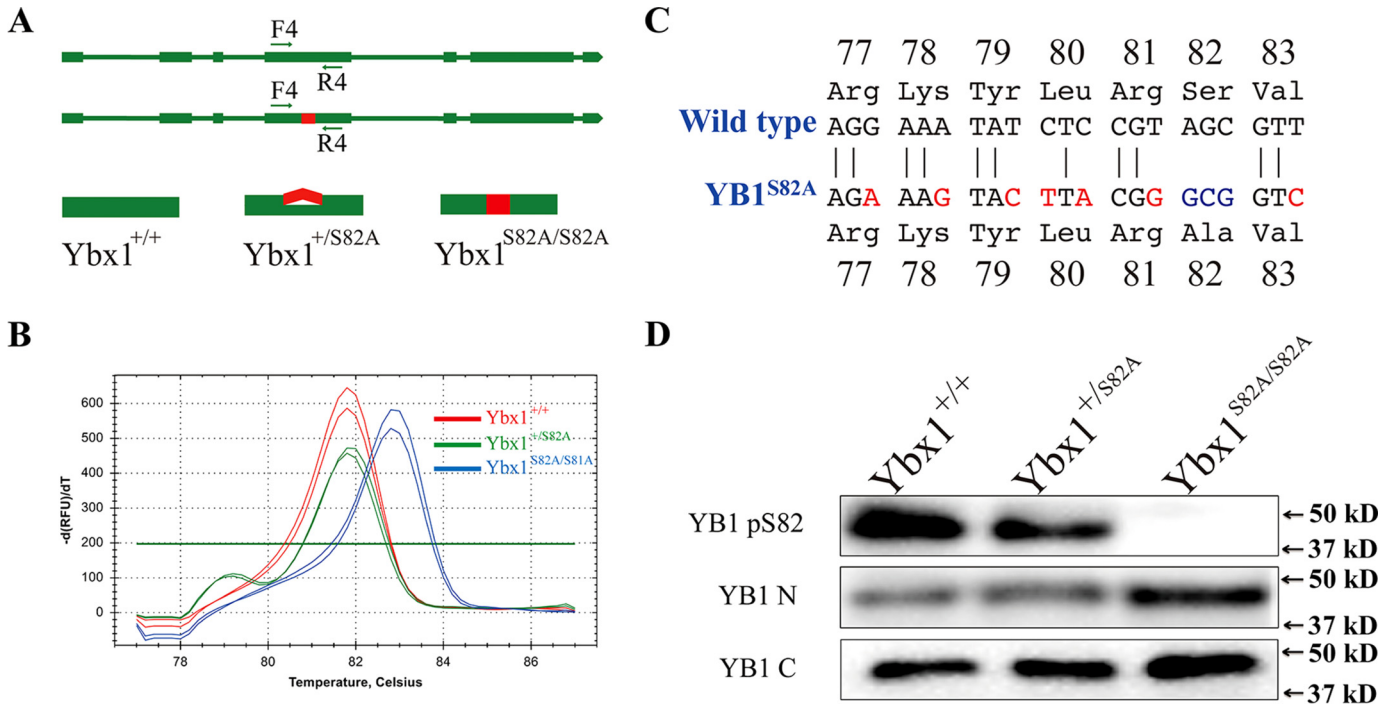

Figure 6. Establishment of homozygous mutant line for Ybx1^{S82A} point mutation. *A*, HRMA-based genotyping with primer pair F4/R4 for identifying Ybx1$^{+/+}$, Ybx1$^{+/S82A}$, and Ybx1$^{S82A/S82A}$. The tail of each larva was cut off for extracting genomic DNA and genotyping. The rest part of the body was frozen for Western blotting assay. *B*, melting curves for WT homozygote (*red*), S82A homozygous mutant (*green*), and heterozygote (*blue*). *C*, sequence confirmation of the homozygous (F2) mutant line for Ybx1^{S82A} point mutation. The amplicon produced with F4/R4 was T/A cloned and sequenced. *D*, detection of Ser-82 phosphorylation in Ybx1$^{+/+}$, Ybx1$^{+/S82A}$, and Ybx1$^{S82A/S82A}$ fish by Western blotting assay. After genotyping, 10 of 4-day post fertilization larvae with the same genotype were pooled together for protein extraction.

we compared Cas9 mRNA and protein in terms of germline transmission rate. Although both Cas9 mRNA and protein showed high efficiency in inducing somatic point mutations in F0 founders, we found only 2 F0 founders with germline transmission from 104 fish injected with Cas9 mRNA (1.9%) (Fig. S4). Interestingly, these 2 F0 fish were identified as negative by caudal fin genotyping (fish *1–2 with 2.8–13.8% transmission rate, percentage of F1 embryos carrying point mutation) (Fig. 4*A*), meaning that they would have been discarded if screened by conventional caudal fin genotyping. In contrast, we identified 7 F0 founders with HDR mutation in their germlines out of 55 fish injected with Cas9 protein (12.7%) (fish #1–7 with 8.3–33.3% transmission rate) (Fig. 4*B*). The details of screening these 55 F0 fish to obtain the 7 positive founders are shown in Fig. S5. Among the 7 founders, 5 fish contained HDR mutation in the caudal fins (#1–5, 9.1%) and 2 fish showed no signal in their caudal fins (#6–7, 3.6%) (Fig. 4*A* and 5*B*). These results suggested a significant improvement of germline transmission of Ybx1^{S82A} point mutation by using Cas9 protein. Our result also showed that although caudal fin genotyping is not reliable to ensure germline transmission, it is helpful to enrich the F0 founders with germline transmission.

Establishment of homozygous mutant line for Ybx1^{S82A} point mutation

To generate homozygous point mutant zebrafish line for Ybx1^{S82A}, we crossed heterozygous F1 fish carrying the point mutation to generate F2 generation, which contained WT (Ybx1$^{+/+}$), heterozygous mutant (Ybx1$^{+/S82A}$), and homozygous mutant (Ybx1$^{S82A/S82A}$). These different genotypes could be easily differentiated by using HRMA with a pair of primers (F4/R4) that flank the mutant site to generate an amplicon of 82 bp (Fig. 6*A*). As shown in Fig. 6*B*, the WT homozygotes generated a single melting peak at 81.7 °C, whereas the peak for S82A homozygous mutant was at 82.8 °C. This difference between WT and mutant could be established and verified at the beginning when the HDR donor was designed. The heterozygotes could be easily distinguished from homozygotes by the shoulder peak at 79.0 °C near the main peak (81.7 °C). The identity of F2 mutant was further confirmed by sequencing, using the amplified products from the homozygotes (Fig. 6*C*).

To further prove that the amino acid Ser-82, which is a critical point for Ybx1 phosphorylation (39), was successfully mutated, we used Western blot analysis to detect phosphorylation at this site with a specific anti–Ser-82 antibody. We used the larvae at 4 days post fertilization (dpf) as the material because a previous study showed that Ybx1 was expressed in the zebrafish during embryonic and post-embryonic stages (46). The tail of each larva was cut off for genotyping with HRMA. Ten larvae with the same genotype were pooled together to extract proteins for Western blot analysis. As shown in Fig. 6*D*, no phosphorylation signal was detected in the homozygous mutant (Ybx1$^{S82A/S82A}$). As controls, both WT and heterozygous mutants showed a strong signal of phosphorylation although the signal was slightly decreased in the heterozygotes. Interestingly, the total Ybx1 protein seemed to be slightly increased in the homozygous mutant as compared with the WT and heterozygotes (Fig. 6*D*).

Discussion

HDR-mediated precise gene editing is a valuable approach for functional analysis and disease modeling. However, the establishment of pure animal lines with specific point mutations is still a challenging task. In this study, we established and validated a highly efficient strategy for generating and establishing zebrafish lines with specific substitutions for single amino acids without loss of the whole proteins.

According to the studies reported so far, one of the limitations for HDR is the poor efficiency, especially *in vivo* at the organism level (18, 47–50). Different approaches have been used to improve HDR efficiency, including different types of DNA donors (22, 23, 51), suppression of the NHEJ pathway or stimulation of the HDR pathway (27, 29, 30), and temporal control of the editing nuclease (52, 53). Although optimization of these parameters improved the efficiency of HDR to different extents, there have been few studies on combination of these approaches for higher efficiency.

ssDNA donor was often reported to be efficient for HDR (12, 23, 54); however, a study from Nüsslein-Volhard's group indicated that plasmid DNA donor increased *in vivo* HDR efficiency to 46% (17). In the present study, we also found that plasmid DNA donor with CRISPR sites produced the highest efficiency among three different donors (ssDNA, dsDNA, and plasmid). One of the reasons could be that depending on sequences, ssDNA donors have a potential to form secondary structures, which may stunt DNA recombination. By comparison, plasmid DNA donors are supposed to be more stable with less sequence-dependent variation.

DNA repair of DSBs involves two pathways, *viz.* NHEJ and HDR. The former often results in indel mutations at the target site, which masks the HDR-induced point mutation in genome editing. One strategy to increase the efficiency of HDR-mediated mutation is to suppress NHEJ or enhance HDR in cells (25, 26). Both SCR7 (NHEJ inhibitor) and RS-1 (HDR enhancer) have been used to improve the HDR rate (27, 29, 30). Our data in the present study showed that treatments of the injected zebrafish embryos with SCR7 or RS-1 could significantly increase the efficiency of HDR for all three types of DNA donors, especially for plasmid donor. Combination of SCR7 and RS-1 further increased HDR rate to 74%, which is the highest efficiency reported so far. Interestingly, we observed that in the absence of DNA donors, SCR7 reduced NHEJ rate as expected; however, its effect was further enhanced by RS-1. This might be because without exogenous DNA donors, the WT allele might serve as the template for the repair through HDR pathway, resulting in reduced NHEJ and increased WT sequence. The presence of RS-1 increases the HDR activity, therefore further enhancing the repair to the WT sequence. When exogenous DNA donors were present, they might compete with the WT allele sequence for repair, resulting in increased HDR-induced point mutation while reducing NHEJ rate. However, the total mutation rates (NHEJ and HDR) remained more or less the same. The third strategy for increasing HDR efficiency is to control the timing of Cas9 expression (52, 53). Because it takes time for Cas9 mRNA to be translated into Cas9 protein, there have been attempts to introduce Cas9 protein directly, instead of mRNA, to increase the success rate of HDR-mediated mutations (55, 56). This is supported by our data in the present study. In contrast to the immediate availability of Cas9 in the embryos after injection of the protein, the Cas9 protein first appeared in the embryos at 8-cell stage after injection of its mRNA at 1-cell stage. This advanced the timing of both NHEJ and HDR, therefore significantly increasing the rate of HDR in various tissues of the F0 fish. This in turn resulted in high germline transmission rate as demonstrated in the present study. In general, the present study provided supportive evidence for the three approaches that have been reported in the literature to enhance HDR-mediated genome editing. In addition, our data suggest that the efficiency of HDR could be further enhanced by different combinations of these parameters. For Ybx1 protein targeted in this study, the best combination was the plasmid DNA donor with Cas9 protein followed by treatment of the injected embryos with SCR7 and RS-1.

Another major limitation for establishing a pure animal line with HDR mutation is the low efficiency of germline transmission (19, 36). It has been reported that the germ materials in the zebrafish start to be detectable at 2-cell stage and become specialized at 4-cell stage. They are concentrated in so-called primordial germ cells (PGCs) from 32-cell stage. These PGC cells undergo asymmetrical mitosis, and their total number maintains constant before 1000-cell stage (57). As a result, the proportion of PGCs keeps decreasing with embryonic development. This suggests that the earlier HDR starts, the higher probability for HDR to occur in the germ cells for transmission to the next generation. Moreover, the embryonic development is much faster in the zebrafish than that in mammals; hence, a little time gap will lead to great difference in editing efficiency in the germline (58). As reported, HDR involves several steps in G_2 phase, and it takes longer time than NHEJ-mediated rapid ligation, which results in reduced efficiency (59). In the present study, we demonstrated that by using Cas9 protein instead of mRNA, the efficiency of HDR germline transmission increased about six times among F0 founders. This could be because of the immediate availability of Cas9 protein in early embryos when the cell number was low, leading to increased chance for editing to occur in the germ cells. A recent study reported that NHEJ could be first detected in 2-cell stage by using Cas9 mRNA; however, they injected very high doses of both Cas9 mRNA and sgRNA directly into the animal pole, making the procedure difficult to operate (60).

Although the three parameters and their combinations could all be optimized for HDR as described above to increase the efficiency of precise genome editing, the second major obstacle for obtaining mutant lines is to detect HDR-mediated mutations and distinguish them from a dizzying number of random indel mutations in the F1 generation. The commonly used genotyping methods, including HRMA, heteroduplex mobility assay (HMA), and T7E1 assay, are all powerful to demonstrate mutations; however, it is difficult to use them to differentiate specific HDR mutations and in particular to separate them from the indel mutations. In the present study, we established an efficient protocol to differentiate F0 individuals that transmitted HDR mutations to the F1 generation even when the

mutation rate was low. The protocol involved several factors. First, when constructing DNA donors, we introduced not only the mutant sequence that changed the amino acid of interest, but also made some base changes nearly without changing amino acids (blocking mutations). This would allow for design of a mutant-specific primer that only detects the mutant sequence introduced by HDR without amplifying indels and WT sequence. Second, we used HRMA for genotyping, which is an efficient and high-throughput genotyping method that could handle large number of samples (61, 62). Third, a device for mass breeding was helpful. In our study, we used iSpawn that allows for breeding of tens of fish at the same time.

In the zebrafish, caudal fin genotyping is the most commonly used method for identifying F0 founder fish that carry somatic mutations. There is usually a good correlation between caudal fin genotyping and germline transmission when the mutation rate is high. However, when the mutation rate is low such as HDR-mediated mutations, the correlation is weak. As shown in the present study, fish without somatic mutations in the fin could still generate mutant fish in the F1 generation. These fish could be identified with our breeding and screening approach. Despite this, our data showed that caudal fin genotyping could still improve the efficiency of screening for F0 individuals that carry HDR mutations.

In conclusion, we established a universal and efficient strategy in the present study for increasing the efficiency of HDR-mediated genome editing in the zebrafish through combination of three different factors, *i.e.* DNA donor design, use of Cas9 protein, and suppression of NHEJ and stimulation of HDR. Furthermore, we developed and validated an efficient method for screening and identifying F0 founder fish that carried and transmitted HDR-mediated mutations. Although we used CRISPR/Cas9 to target Ybx1 protein in the present study, the platform established can be applied to other genes and other genome editing methods such as TALEN and zinc finger nuclease. This will greatly facilitate functional study of genes at molecular level and modeling of human genetic diseases, which often involve point mutations rather than the loss of whole proteins.

Experimental procedures

Zebrafish and maintenance

The AB strain zebrafish was used for generating mutant lines. The fish were maintained in the ZebTEC multilinking rack system (Tecniplast, Buguggiate, Italy) under a constant condition (photoperiod: 14 h light/10 h dark; temperature: 28 ± 1 °C; pH: 7.5; and conductivity: 400 microsiemens/centimeter). The breeding was set up in a 1-liter breeding box (Tecniplast) for pair/small-group breeding or in iSpawn (Tecniplast) for large-group mass breeding. The fish fry were raised in the Forma Environmental Chamber (Model 3949, Thermo Scientific) with paramecia and transferred to the ZebTEC multilinking rack zebrafish system after starting to feed on *Artemia*. The fish were fed twice a day with Otohime fish diet (Marubeni Nisshin Feed, Tokyo, Japan) by the Tritone automatic feeding system (Tecniplast). All the experiments performed in this study were approved by the Research Ethics Committee of University of Macau.

Synthesis of sgRNA, Cas9 mRNA, and TALEN mRNA

CRISPR/Cas9 and TALEN target sites were identified by the online ZiFiT Targeter software (http://zifit.partners.org/ZiFiT)[4] (64, 65). Site 1 (GCTACGGAGATATTTCCTCGGG) and site 2 (GGAAATATCCGTAGCGTTGGG) near the Ser-82 codon were used for CRISPR/Cas9 system, and the sites for left and right TALEs were TAAAAAGAACAACCCC-AGGA and TCCACAGTCTCTCCGTC, respectively. The annealed oligonucleotides were ligated into the BsaI-cleaved sgRNA vector pDR274 (Addgene, Cambridge, MA). The plasmids for sgRNAs were then digested by DraI and used as templates for *in vitro* transcription using the MEGAscript T7 kit (Life Technologies). The left and right TALEs were assembled by using the Golden Gate Kit (Addgene). The capped mRNAs for Cas9 were transcribed from zebrafish codon-optimized pCS2-nCas9n plasmid (Addgene). The pCS2-nCas9n plasmid (for Cas9 mRNA) and pTAL1 plasmids (for left and right TALE mRNAs) were linearized by NotI followed by *in vitro* transcription using mMESSAGE SP6 kit (Life Technologies). The concentrations of the sgRNA and capped mRNAs were measured by NanoDrop (Thermo Scientific) and its quality was examined by agarose gel electrophoresis (61). The Cas9 protein was purchased from PNA Bio (Newbury Park, CA).

Donor assembly

The homologous arms of HDR donors were amplified from zebrafish genomic DNA with primers Fd1/Rm1 and Fm1/Rd1, respectively (Fig. 1*C*). Mutations were introduced at the 5′-end of the primers Fm1 and Rm1. The left and right homologous arms were linked by fusion PCR with Fd1 and Rd1. For plasmid DNA donor, the CRISPR target site and PAM sequence were introduced to flank the homologous region with primers FdC1 and RdC1, followed by TA cloning (Takara Bio, Shiga, Japan). All primers used in this study were synthesized by IDT (Table S1).

Microinjection

The 5′-capped Cas9 mRNA (200 ng/μl) or Cas9 protein (200 ng/μl) was mixed with sgRNA (50 ng/μl) and HDR donor DNA (200 ng/μl), and co-injected into the yolk of 1-cell zebrafish embryos at the total volume of 4.6 nl/embryo using the Drummond Nanoject system (Drummond Scientific, Broomall, PA) (61). The injected embryos were then incubated in 20 μM SCR7 (Xcess Biosciences, San Diego, CA) and 20 μM RS-1 (Sigma) alone or in combination for 6 h. The same amount of vehicle DMSO (Sigma) was used as the control. The treatment solutions were then replaced by system water (Fig. 1*A*).

Genomic DNA extraction

The genomic DNA was extracted using the HotSHOT method (63). Briefly, the whole embryo or a piece of tissue such as caudal/tail fin was incubated in 50 μl NaOH (50 mM) at 95 °C for 10 min. The solution was then cooled to room temperature and neutralized with 1/10 volume Tris-HCl (1 M, pH 8.0). The samples were centrifuged at 15,000 rpm for 1 min, and the

supernatants were ready for genotyping. For genomic DNA samples from 1- to 128-cell embryos, the supernatants were subject to vacuum concentration until drying. The PCR mix was then added into each sample tube, incubated for 15 min at room temperature, and transferred to the PCR plate.

High-resolution melting analysis– based genotyping

We used HRMA to detect mutations resulting from CRISPR-induced DSBs (60, 61). Briefly, a 170-bp amplicon that included target site was generated with the primers (F0 and R0) (Fig. S1) flanking the target site in a 10-μl PCR reaction, which contained 5 μl Precision Melt Supermix (Bio-Rad), 2 μl genomic DNA from embryos or fin cuts, and 400 nM each forward and reverse primers. The conditions for amplification were as follows: denaturation at 95 °C for 3 min, 40 cycles of reaction at 95 °C for 15 s, annealing at 55 °C for 20 s, and extension at 72 °C for 2 min. The melt curve analysis was performed after amplification as follows: denaturation first at 95 °C for 15 s, decreasing temperature from 95 to 70 °C for annealing or duplex formation, and curve melting from 70 to 95 °C with 0.2 °C increment each step. The amplification was performed on the CFX96 real-time PCR system (Bio-Rad). The HRMA profile for each gene was presented as a melt peak. For genotyping the F2 generation, primers F4 and R4 were used to generate a shorter amplicon (82 bp) (Fig. 6*A*), which was sensitive enough to distinguish different genotypes (WT/WT, WT/S82A, and S82A/S82A).

Genotyping for HDR-induced site-specific mutations

To distinguish HDR mutations from large amount of background indel mutations, a primer (R2) that specifically recognizes mutant sequence introduced by HDR was designed to work with primer F2 (Fig. 1*D*). To optimize the real-time PCR condition, we tested a gradient annealing temperature from 55 to 65 °C to optimize the condition that could distinguish the HDR-induced mutation from the WT and random indel mutations. The amplification conditions were as follows: denaturation at 95 °C for 3 min, 40 cycles of reaction at 95 °C for 15 s, annealing at 60 °C for 20 s, and extension at 72 °C for 1 min and 30 s. To exclude the interference by the residual HDR donors remaining in the reaction, nested PCR was employed. Briefly, the first round of PCR was performed with F1 and R1, which are located outside the region of the donor DNAs. The products were then diluted 200 times and 2 μl diluted reaction was used for the second round of PCR with F2 and R2. The mutant-specific primer R2 ensures that only the HDR-induced mutant sequence is amplified (Fig. 1*D*).

To detect the HDR and NHEJ mutations in early embryonic stages (1–128 cells), an additional pair of primers (F3 and R3) located outside the HDR template was used for the first round of PCR because the cell number was often too low to generate significant signals (Fig. 2*B*). The condition for the first amplification (F3 and R3) was as follows: denaturation at 95 °C for 3 min followed by 40 cycles of reaction (denaturation at 95 °C for 15 s, annealing at 55 °C for 20 s, and extension at 72 °C for 2 min). The second amplification for detecting HDR mutation (F1 and R2) was performed as follows: denaturation at 95 °C for 3 min followed by 40 cycles of reaction (denaturation at 95 °C for 15 s, annealing at 60 °C for 20 s, and extension at 72 °C for 1 min). The products were then examined by agarose electrophoresis (0.8%). For detecting the NHEJ mutations, the second amplification was performed with F1 and R1 at the following condition: denaturation at 95 °C for 3 min followed by 40 cycles of reaction (denaturation at 95 °C for 15 s, annealing at 55 °C for 20 s, and extension at 72 °C for 1 min and 30 s). The products were purified with the QIAquick PCR Purification Kit (Qiagen, Valencia, CA) and subject to digestion with T7 Endonuclease I (T7E1 assay) (New England Biolabs, Ipswich, MA). Both digested and undigested products were subject to agarose electrophoresis (0.8%).

Screening for germline transmission of HDR-induced mutations

In this study, we developed an efficient protocol that enabled us to differentiate F0 founder fish that could transmit point mutations to the offspring regardless of the efficiency of HDR. First, we did a mass breeding among all the F0 founders in the iSpawn (Tecniplast) and collected the F1 embryos. The embryos were pooled and grouped at 50 or less per group. Genomic DNA was then extracted from the grouped embryos for detection of HDR-induced mutations as described above. If no signal was detected in any groups, the F0 fish tested were discarded. If positive signals were detected in any group, the F0 founders were then divided into two groups for a new round of mass breeding within each group to enrich the F0 fish that showed germline transmission with positive F1 individuals. This kind of grouping, breeding, and screening was repeated with decreasing group size of F0 fish in every cycle until the number reached 10 or less per group. The last 10 or less individuals from the final group that showed positive signals were then tested by individual breeding with WT fish (Fig. 5*A*).

Western blotting

We used Western blotting to monitor the expression of proteins and the success of the point mutation in the embryos (for Cas9) or larvae (for Ybx1 and phospho-Ybx1). To extract proteins from embryos, 50 embryos at the same developmental stage were collected each time followed by removing the chorion and yolk according to the procedure described in *The Zebrafish Book* (66). For larval fish, each fish was genotyped first on tail fin DNA followed by protein extraction from the rest of the body. The proteins from 50 embryos or 10 larvae per sample were then separated by SDS-PAGE (10%) and transferred to polyvinylidene difluoride (PVDF) membrane (EMD Millipore) for probing. Each membrane was blocked by incubating in 5% BSA in 1× TBST followed by probing with the first antibodies at 4 °C overnight. We used our homemade zebrafish-specific anti-Ybx1 (YB1N for N-terminal, and YB1C for C-terminal) (GenScript, Nanjing, China) to detect total Ybx1, and an anti–phospho-Ybx1 (pS82) from Cell Signaling Technology (no. 2900, Danvers, MA) to detect phosphorylation at Ser-82. The expression of Cas9 was monitored with an anti-Cas9 (no. 14697, Cell Signaling Technology). After incubation with the first antibodies, each membrane was then washed with 1× TBST three times fol-

lowed by incubation with a HRP-labeled secondary antibody (no. 31460, Thermo Fisher). After washing with 1× TBST, the signals were developed using the SuperSignal ECL kit (Thermo Scientific).

Statistical analysis

All values were expressed as mean ± S.E., and the data were analyzed by ANOVA followed by Tukey's test using Prism 6 on Macintosh OS X (GraphPad Software, San Diego, CA).

Author contributions—Y. Z. and W. G. conceptualization; Y. Z. data curation; Y. Z. and W. G. formal analysis; Y. Z. validation; Y. Z. and Z. Z. investigation; Y. Z. visualization; Y. Z. and Z. Z. methodology; Y. Z. and W. G. writing-original draft; Y. Z. and W. G. writing-review and editing; W. G. resources; W. G. software; W. G. supervision; W. G. funding acquisition; W. G. project administration.

References

1. Hsu, P. D., Lander, E. S., and Zhang, F. (2014) Development and applications of CRISPR-Cas9 for genome engineering. *Cell* **157,** 1262–1278 CrossRef Medline
2. Boch, J., Scholze, H., Schornack, S., Landgraf, A., Hahn, S., Kay, S., Lahaye, T., Nickstadt, A., and Bonas, U. (2009) Breaking the code of DNA binding specificity of TAL-type III effectors. *Science* **326,** 1509–1512 CrossRef Medline
3. Vannocci, T., Faggianelli, N., Zaccagnino, S., della Rosa, I., Adinolfi, S., and Pastore, A. (2015) A new cellular model to follow Friedreich's ataxia development in a time-resolved way. *Dis. Model. Mech.* **8,** 711–719 CrossRef Medline
4. Chen, Y., Zheng, Y., Kang, Y., Yang, W., Niu, Y., Guo, X., Tu, Z., Si, C., Wang, H., Xing, R., Pu, X., Yang, S. H., Li, S., Ji, W., and Li, X. J. (2015) Functional disruption of the dystrophin gene in rhesus monkey using CRISPR/Cas9. *Hum. Mol. Genet.* **24,** 3764–3774 CrossRef Medline
5. Schmid, B., and Haass, C. (2013) Genomic editing opens new avenues for zebrafish as a model for neurodegeneration. *J. Neurochem.* **127,** 461–470 CrossRef Medline
6. Guo, X., Wang, X., Wang, Z., Banerjee, S., Yang, J., Huang, L., and Dixon, J. E. (2016) Site-specific proteasome phosphorylation controls cell proliferation and tumorigenesis. *Nat. Cell Biol.* **18,** 202–212 CrossRef Medline
7. Shinkuma, S., Guo, Z., and Christiano, A. M. (2016) Site-specific genome editing for correction of induced pluripotent stem cells derived from dominant dystrophic epidermolysis bullosa. *Proc. Natl. Acad. Sci. U.S.A.* **113,** 5676–5681 CrossRef Medline
8. Steentoft, C., Bennett, E. P., Schjoldager, K. T., Vakhrushev, S. Y., Wandall, H. H., and Clausen, H. (2014) Precision genome editing: A small revolution for glycobiology. *Glycobiology* **24,** 663–680 CrossRef Medline
9. Hanahan, D., and Weinberg, R. A. (2011) Hallmarks of cancer: The next generation. *Cell* **144,** 646–674 CrossRef Medline
10. Sueda, T., Sakai, D., Kawamoto, K., Konno, M., Nishida, N., Koseki, J., Colvin, H., Takahashi, H., Haraguchi, N., Nishimura, J., Hata, T., Takemasa, I., Mizushima, T., Yamamoto, H., Satoh, T., Doki, Y., Mori, M., and Ishii, H. (2016) BRAF(V600E) inhibition stimulates AMP-activated protein kinase-mediated autophagy in colorectal cancer cells. *Sci. Rep.* **6,** 18949 CrossRef Medline
11. Fiala, O., Buchler, T., Mohelnikova-Duchonova, B., Melichar, B., Matejka, V. M., Holubec, L., Kulhankova, J., Bortlicek, Z., Bartouskova, M., Liska, V., Topolcan, O., Sedivcova, M., and Finek, J. (2016) G12V and G12A KRAS mutations are associated with poor outcome in patients with metastatic colorectal cancer treated with bevacizumab. *Tumour Biol.* **37,** 6823–6830 CrossRef Medline
12. Wang, X., Wang, Y., Huang, H., Chen, B., Chen, X., Hu, J., Chang, T., Lin, R. J., and Yee, J. K. (2014) Precise gene modification mediated by TALEN and single-stranded oligodeoxynucleotides in human cells. *PLoS One* **9,** e93575 CrossRef Medline
13. Davis, L., and Maizels, N. (2014) Homology-directed repair of DNA nicks via pathways distinct from canonical double-strand break repair. *Proc. Natl. Acad. Sci. U.S.A.* **1,** E924–E932 CrossRef Medline
14. Auer, T. O., Duroure, K., De Cian, A., Concordet, J. P., and Del Bene, F. (2014) Highly efficient CRISPR/Cas9-mediated knock-in in zebrafish by homology-independent DNA repair. *Genome Res.* **24,** 142–153 CrossRef Medline
15. Auer, T. O., and Del Bene, F. (2014) CRISPR/Cas9 and TALEN-mediated knock-in approaches in zebrafish. *Methods* **69,** 142–150 CrossRef Medline
16. Ablain, J., Durand, E. M., Yang, S., Zhou, Y., and Zon, L. I. (2015) A CRISPR/Cas9 vector system for tissue-specific gene disruption in zebrafish. *Dev. Cell* **32,** 756–764 CrossRef Medline
17. Irion, U., Krauss, J., and Nüsslein-Volhard, C. (2014) Precise and efficient genome editing in zebrafish using the CRISPR/Cas9 system. *Development* **141,** 4827–4830 CrossRef Medline
18. Shin, J., Chen, J., and Solnica-Krezel, L. (2014) Efficient homologous recombination-mediated genome engineering in zebrafish using TALE nucleases. *Development* **141,** 3807–3818 CrossRef Medline
19. Shah, A. N., and Moens, C. B. (2016) Approaching perfection: New developments in zebrafish genome engineering. *Dev. Cell* **36,** 595–596 CrossRef Medline
20. Armstrong, G. A., Liao, M., You, Z., Lissouba, A., Chen, B. E., and Drapeau, P. (2016) Homology directed knockin of point mutations in the zebrafish *tardbp* and *fus* genes in ALS using the CRISPR/Cas9 system. *PLoS One* **11,** e0150188 CrossRef Medline
21. Port, F., Chen, H. M., Lee, T., and Bullock, S. L. (2014) Optimized CRISPR/Cas tools for efficient germline and somatic genome engineering in *Drosophila*. *Proc. Natl. Acad. Sci. U.S.A.* **111,** E2967–E2976 CrossRef Medline
22. Petrezselyova, S., Kinsky, S., Truban, D., Sedlacek, R., Burtscher, I., and Lickert, H. (2015) Homology arms of targeting vectors for gene insertions and CRISPR/Cas9 technology: Size does not matter; quality control of targeted clones does. *Cell. Mol. Biol. Lett.* **20,** 773–787 CrossRef Medline
23. Richardson, C. D., Ray, G. J., DeWitt, M. A., Curie, G. L., and Corn, J. E. (2016) Enhancing homology-directed genome editing by catalytically active and inactive CRISPR-Cas9 using asymmetric donor DNA. *Nat. Biotechnol.* **34,** 339–344 CrossRef Medline
24. Pinder, J., Salsman, J., and Dellaire, G. (2015) Nuclear domain 'knock-in' screen for the evaluation and identification of small molecule enhancers of CRISPR-based genome editing. *Nucleic Acids Res.* **43,** 9379–9392 CrossRef Medline
25. Vartak, S. V., and Raghavan, S. C. (2015) Inhibition of nonhomologous end joining to increase the specificity of CRISPR/Cas9 genome editing. *FEBS J.* **282,** 4289–4294 CrossRef Medline
26. Yu, C., Liu, Y., Ma, T., Liu, K., Xu, S., Zhang, Y., Liu, H., La Russa, M., Xie, M., Ding, S., and Qi, L. S. (2015) Small molecules enhance CRISPR genome editing in pluripotent stem cells. *Cell Stem Cell* **16,** 142–147 CrossRef Medline
27. Song, J., Yang, D., Xu, J., Zhu, T., Chen, Y. E., and Zhang, J. (2016) RS-1 enhances CRISPR/Cas9- and TALEN-mediated knock-in efficiency. *Nat. Commun.* **7,** 10548 CrossRef Medline
28. Jayathilaka, K., Sheridan, S. D., Bold, T. D., Bochenska, K., Logan, H. L., Weichselbaum, R. R., Bishop, D. K., and Connell, P. P. (2008) A chemical compound that stimulates the human homologous recombination protein RAD51. *Proc. Natl. Acad. Sci. U.S.A.* **105,** 15848–15853 CrossRef Medline
29. Chu, V. T., Weber, T., Wefers, B., Wurst, W., Sander, S., Rajewsky, K., and Kühn, R. (2015) Increasing the efficiency of homology-directed repair for CRISPR-Cas9-induced precise gene editing in mammalian cells. *Nat. Biotechnol.* **33,** 543–548 CrossRef Medline
30. Maruyama, T., Dougan, S. K., Truttmann, M. C., Bilate, A. M., Ingram, J. R., and Ploegh, H. L. (2015) Increasing the efficiency of precise genome editing with CRISPR-Cas9 by inhibition of nonhomologous end joining. *Nat. Biotechnol.* **33,** 538–542 CrossRef Medline
31. Varshney, G. K., Sood, R., and Burgess, S. M. (2015) Understanding and editing the zebrafish genome. *Adv. Genet.* **92,** 1–52 CrossRef Medline

32. Gupta, A., Hall, V. L., Kok, F. O., Shin, M., McNulty, J. C., Lawson, N.D., and Wolfe, S. A. (2013) Targeted chromosomal deletions and inversions in zebrafish. *Genome Res.* **23,** 1008–1017 CrossRef Medline
33. Ota, S., and Kawahara, A. (2014) Zebrafish: A model vertebrate suitable for the analysis of human genetic disorders. *Congenit. Anom. (Kyoto)* **54,** 8–11 CrossRef Medline
34. Huang, P., Xiao, A., Tong, X., Zu, Y., Wang, Z., and Zhang, B. (2014) TALEN construction via "Unit Assembly" method and targeted genome modifications in zebrafish. *Methods* **69,** 67–75 CrossRef Medline
35. Howe, K., Clark, M. D., Torroja, C. F., Torrance, J., Berthelot, C., Muffato, M., Collins, J. E., Humphray, S., McLaren, K., Matthews, L., McLaren, S., Sealy, I., Caccamo, M., Churcher, C., Scott, C., et al. (2013) The zebrafish reference genome sequence and its relationship to the human genome. *Nature* **496,** 498–503 CrossRef Medline
36. Hoshijima, K., Jurynec, M. J., and Grunwald, D. J. (2016) Precise editing of the zebrafish genome made simple and efficient. *Dev. Cell* **36,** 654–667 CrossRef Medline
37. Zhu, B., and Ge, W. (2018) Genome editing in fishes and their applications. *Gen. Comp. Endocrinol.* **257,** 3–12 CrossRef Medline
38. Mao, P., Liu, J., Zhang, Z., Zhang, H., Liu, H., Gao, S., Rong, Y. S., and Zhao, Y. (2016) Homologous recombination-dependent repair of telomeric DSBs in proliferating human cells. *Nat. Commun.* **7,** 12154 CrossRef Medline
39. Lyabin, D. N., Eliseeva, I. A., and Ovchinnikov, L. P. (2014) YB-1 protein: Functions and regulation. *Wiley Interdiscip. Rev. RNA* **5,** 95–110 CrossRef Medline
40. Symington, L. S., and Gautier, J. (2011) Double-strand break end resection and repair pathway choice. *Annu. Rev. Genet.* **45,** 247–271 CrossRef Medline
41. Bedell, V. M., and Ekker, S. C. (2015) Using engineered endonucleases to create knockout and knockin zebrafish models. *Methods Mol. Biol.* **1239,** 291–305 CrossRef Medline
42. Paix, A., Folkmann, A., Rasoloson, D., and Seydoux, G. (2015) High efficiency, homology-directed genome editing in *Caenorhabditis elegans* using CRISPR-Cas9 ribonucleoprotein complexes. *Genetics* **201,** 47–54 CrossRef Medline
43. Wang, B., Li, K., Wang, A., Reiser, M., Saunders, T., Lockey, R. F., and Wang, J. W. (2015) Highly efficient CRISPR/HDR-mediated knock-in for mouse embryonic stem cells and zygotes. *Biotechniques* **59,** 201–202, 204, 206–208 CrossRef Medline
44. Burger, A., Lindsay, H., Felker, A., Hess, C., Anders, C., Chiavacci, E., Zaugg, J., Weber, L. M., Catena, R., Jinek, M., Robinson, M. D., and Mosimann, C. (2016) Maximizing mutagenesis with solubilized CRISPR-Cas9 ribonucleoprotein complexes. *Development* **143,** 2025–2037 CrossRef Medline
45. Takaoka, K., and Hamada, H. (2012) Cell fate decisions and axis determination in the early mouse embryo. *Development* **139,** 3–14 CrossRef Medline
46. Kumari, P., Gilligan, P. C., Lim, S., Tran, L. D., Winkler, S., Philp, R., and Sampath, K. (2013) An essential role for maternal control of Nodal signaling. *eLife* **2,** e00683 CrossRef Medline
47. Ahrabi, S., Sarkar, S., Pfister, S. X., Pirovano, G., Higgins, G. S., Porter, A. C., and Humphrey, T. C. (2016) A role for human homologous recombination factors in suppressing microhomology-mediated end joining. *Nucleic Acids Res.* **44,** 5743–5757 CrossRef Medline
48. Voit, R. A., Hendel, A., Pruett-Miller, S. M., and Porteus, M. H. (2014) Nuclease-mediated gene editing by homologous recombination of the human globin locus. *Nucleic Acids Res.* **42,** 1365–1378 CrossRef Medline
49. Ponce de León, V., Mérillat, A. M., Tesson, L., Anegón, I., and Hummler, E. (2014) Generation of TALEN-mediated GR^{dim} knock-in rats by homologous recombination. *PLoS One* **9,** e88146 CrossRef Medline
50. Cui, C., Song, Y., Liu, J., Ge, H., Li, Q., Huang, H., Hu, L., Zhu, H., Jin, Y., and Zhang, Y. (2015) Gene targeting by TALEN-induced homologous recombination in goats directs production of β-lactoglobulin-free, high-human lactoferrin milk. *Sci. Rep.* **5,** 10482 CrossRef Medline
51. Renaud, J. B., Boix, C., Charpentier, M., De Cian, A., Cochennec, J., Duvernois-Berthet, E., Perrouault, L., Tesson, L., Edouard, J., Thinard, R., Cherifi, Y., Menoret, S., Fontanière, S., de Crozé, N., Fraichard, A., Sohm, F., Anegon, I., Concordet, J. P., and Giovannangeli, C. (2016) Improved genome editing efficiency and flexibility using modified oligonucleotides with TALEN and CRISPR-Cas9 nucleases. *Cell Rep.* **14,** 2263–2272 CrossRef Medline
52. Gutschner, T., Haemmerle, M., Genovese, G., Draetta, G. F., and Chin, L. (2016) Post-translational regulation of Cas9 during G1 enhances homology-directed repair. *Cell Rep.* **14,** 1555–1566 CrossRef Medline
53. Lin, S., Staahl, B. T., Alla, R. K., and Doudna, J. A. (2014) Enhanced homology-directed human genome engineering by controlled timing of CRISPR/Cas9 delivery. *eLife* **3,** e04766 CrossRef Medline
54. Sauer, N. J., Mozoruk, J., Miller, R. B., Warburg, Z. J., Walker, K. A., Beetham, P. R., Schöpke, C. R., and Gocal, G. F. (2016) Oligonucleotide-directed mutagenesis for precision gene editing. *Plant Biotechnol. J.* **14,** 496–502 CrossRef Medline
55. Ménoret, S., De Cian, A., Tesson, L., Remy, S., Usal, C., Boulé, J. B., Boix, C., Fontanière, S., Crénéguy, A., Nguyen, T. H., Brusselle, L., Thinard, R., Gauguier, D., Concordet, J. P., Cherifi, Y., Fraichard, A., Giovannangeli, C., and Anegon, I. (2015) Homology-directed repair in rodent zygotes using Cas9 and TALEN engineered proteins. *Sci. Rep.* **5,** 14410 CrossRef Medline
56. Ma, Y., Chen, W., Zhang, X., Yu, L., Dong, W., Pan, S., Gao, S., Huang, X., and Zhang, L. (2016) Increasing the efficiency of CRISPR/Cas9-mediated precise genome editing in rats by inhibiting NHEJ and using Cas9 protein. *RNA Biol.* **13,** 605–612 CrossRef Medline
57. Raz, E. (2003) Primordial germ-cell development: The zebrafish perspective. *Nat. Rev. Genet.* **4,** 690–700 CrossRef Medline
58. Kimmel, C. B., Ballard, W. W., Kimmel, S. R., Ullmann, B., and Schilling, T. F. (1995) Stages of embryonic development of the zebrafish. *Dev. Dyn.* **203,** 253–310 CrossRef Medline
59. Orthwein, A., Noordermeer, S. M., Wilson, M. D., Landry, S., Enchev, R. I., Sherker, A., Munro, M., Pinder, J., Salsman, J., Dellaire, G., Xia, B., Peter, M., and Durocher, D. (2015) A mechanism for the suppression of homologous recombination in G1 cells. *Nature* **528,** 422–426 CrossRef Medline
60. Samarut, É., Lissouba, A., and Drapeau, P. (2016) A simplified method for identifying early CRISPR-induced indels in zebrafish embryos using high resolution melting analysis. *BMC Genomics* **17,** 547 CrossRef Medline
61. Zhang, Z., Zhu, B., and Ge, W. (2015) Genetic analysis of zebrafish gonadotropin (FSH and LH) functions by TALEN-mediated gene disruption. *Mol. Endocrinol.* **29,** 76–98 CrossRef Medline
62. Dahlem, T. J., Hoshijima, K., Jurynec, M. J., Gunther, D., Starker, C. G., Locke, A. S., Weis, A. M., Voytas, D. F., and Grunwald, D. J. (2012) Simple methods for generating and detecting locus-specific mutations induced with TALENs in the zebrafish genome. *PLoS Genet.* **8,** e1002861 CrossRef Medline
63. Truett, G. E., Heeger, P., Mynatt, R. L., Truett, A. A., Walker, J. A., and Warman, M. L. (2000) Preparation of PCR-quality mouse genomic DNA with hot sodium hydroxide and Tris (HotSHOT). *Biotechniques* **29,** 52, 54 Medline
64. Sander, J.D., Zaback, P.Z., Joung, J.K., Voytas, D.F., Dobbs, D. (2007) Zinc finger targeter (ZiFiT): An engineered zinc finger/target site design tool. *Nucleic Acids Res.* **35,** W599–W605 CrossRef Medline
65. Sander, J.D., Maeder, M.L., Reyon, D., Voytas, D.F., Joung, J.K., Dobbs, D. (2010) ZiFiT (zinc finger targeter): An updated zinc finger engineering tool. *Nucleic Acids Res.* **38,** W462–W468 CrossRef Medline
66. Westerfield, M. (2000). *The Zebrafish Book. A Guide for The Laboratory Use of Zebrafish* (*Danio rerio*), 4th ed. University of Oregon Press, Eugene, OR

ASBMB